



e 420294

AIAA – 99 - 3505

**JET SPREADING INCREASE BY PASSIVE
CONTROL AND ASSOCIATED PERFORMANCE
PENALTY**

K. B. M. Q. Zaman
NASA Glenn Research Center
Cleveland, OH 44135

30th AIAA Fluid Dynamics Conference
28 June - 1 July, 1999 / Norfolk, VA

JET SPREADING INCREASE BY PASSIVE CONTROL AND ASSOCIATED PERFORMANCE PENALTY

by

K. B. M. Q. Zaman
NASA Glenn Research Center
Cleveland, OH 44135

Abstract

This paper reviews the effects of 'screech', 'asymmetric nozzle shaping', 'tabs' and 'overexpansion' on the spreading of free jets. Corresponding thrust penalty for the tabs and overexpanded condition are also evaluated. The asymmetric shapes include rectangular ones with varying aspect ratio. Tabs investigated are triangular shaped 'delta-tabs' placed at the exit of a convergent circular nozzle. The effect of overexpansion is examined with circular convergent-divergent (C-D) nozzles. Tabs and overexpansion are found to yield the largest increase in jet spreading. Each, however, involves a performance penalty, i.e., a loss in thrust coefficient. Variation of the size of four delta-tabs show that there exists an optimum size for which the gain in jet spreading is the maximum per unit loss in thrust coefficient. With the C-D nozzles, the minimum in thrust coefficient is expected near the beginning of the overexpanded regime based on idealized flow calculations. The maximum increase in jet spreading, however, is found to occur at higher pressure ratios well into the overexpanded regime. The optimum benefit with the overexpanded flow, in terms of gain in spreading for unit penalty, is found to be comparable to the optimum tab case.

1. Introduction

An increase in jet spreading is desired in many applications for a variety of reasons. This has led to extensive research seeking methods for jet mixing enhancement. Unfortunately, methods that yield a significant increase in jet spreading are also typically accompanied by a performance penalty, i.e., a loss in thrust coefficient. While some penalty may be acceptable in

many situations it is of critical concern in propulsion applications. This paper reviews the gain in jet spreading and the corresponding loss in thrust coefficient associated with several 'passive control' techniques.

Flow control techniques investigated in the past include the use of non-axisymmetric nozzle shaping (rectangular, elliptic, etc.), lobed nozzles, vortex generators, beveled nozzles, as well as natural and induced flow resonance. Gutmark et al.¹ provided a review of the earlier investigations. However, there was a difficulty in directly comparing the spreading increase achieved by the various techniques. A variety of criteria had been employed in the previous studies to characterize jet entrainment and spreading. These included mean velocity or mean temperature at a given downstream location, shear layer thickness, jet half-velocity-widths on major and minor axes, etc.; see, for example, the list of "measure of enhancement" in table 1 of Ref. 1. Other parameters (e.g., jet Mach number) also varied from experiment to experiment, making it difficult, if not impossible, to compare the effects. It was also clear that a full assessment of the spreading for the non-axisymmetric jets would require detailed survey of the flow field in three-dimensional space. These considerations led to an effort by the author and colleagues that was initiated several years ago. The jet spreading was assessed on the basis of detailed Pitot probe surveys and quantified based on variations of longitudinal mass flow rate. The effects of nozzle shaping, vortex generators, screech, etc., were examined. The results, obtained so far, have been summarized recently (Ref. 2). Some of those results are reviewed in the present paper.

While the increase of jet spreading by various methods has been addressed in many previous investigations, the corresponding thrust penalty has been addressed by relatively a few. This is an important issue especially in

propulsion applications. This is addressed in the present paper with available data and analysis.

An operating parameter that affects jet spreading but has gone practically unnoticed in previous studies is the state of overexpansion with convergent-divergent nozzles. Overexpansion refers to an off-design operating pressure lower than the design pressure for a C-D nozzle. It can lead to a faster jet spreading. The effect has been noted by Professor D. Papamoschou of University of California, Irvine, (private communication). It can also be observed in earlier data sets, e.g., those presented in connection with asymptotic spreading rates of initially compressible jets (Ref. 3; figure 7). This effect is addressed in detail with data obtained recently from two C-D nozzles. There is a thrust penalty associated with overexpansion. The loss in thrust coefficient is calculated using idealized one-dimensional nozzle flow analysis. In the following, these new results are presented as part of an overview of the subject under consideration.

2. Experimental Method

The details of the experimental procedures for the data presented in the following have been discussed in earlier publications (Ref. 2); these are briefly summarized here. The data were obtained in two open jet facilities. For all data, the total temperature in the plenum chamber equaled that of the ambient. The jet discharged into the quiescent ambient of the laboratory. In the following, the 'jet Mach number' (M_j) is used as an independent variable. It represents the Mach number at the nozzle exit had the flow expanded fully and is related to the pressure ratio through the equation,

$$M_j = \left(\left(\frac{p_0}{p_a} \right)^{\frac{\gamma-1}{\gamma}} - 1 \right)^{1/2} \frac{2}{\gamma-1}, \text{ where } \gamma \text{ is the}$$

ratio of specific heats, and p_0 and p_a are plenum chamber and ambient pressures, respectively.

The asymmetric nozzles included a 3:1 elliptic, a 3:1 rectangular and a 6-lobed case. The equivalent diameter (D_e), based on nozzle exit cross-sectional area, was the same for all, 1.47 cm. The tabs used were 'delta-tabs' (Ref. 2), having triangular shapes with base on the nozzle wall and the plane of the tab making an angle of about 45° with the jet axis. Only four equally

spaced delta-tabs placed at the exit of the circular nozzle are considered here. The size of the tabs for the given nozzle was varied in an effort to determine the optimum size.

In addition to the rectangular and elliptic nozzles, data were also obtained for a set of rectangular orifices. The aspect ratio was varied as, 1:1, 2:1, 4:1, 8:1, 16:1 and 32:1, keeping the exit area the same. The corresponding equivalent diameter was 2.54 cm. These data allowed an assessment of the effect of 'shear layer perimeter stretching' on jet mixing enhancement. The entrance of each orifice was faired with a radius of curvature of about 5 mm, the orifice plate thickness was 6.35 mm.

Data on the effect of overexpansion were obtained with two circular, C-D nozzles, each having an exit diameter (D_e) of 2.54 cm. The design Mach numbers (M_D) for the two were 1.4 and 1.8. The throat diameters (D_t) for the two were 2.41 cm and 2.12 cm, and throat-to-exit lengths were 2.2 cm and 3.45 cm, respectively. Detailed interior profiles can be found in Ref. 4.

The Pitot probe surveys were conducted under automated computer control. A rake of three probes was used to reduce data acquisition time. All data were acquired far enough downstream where the flow was fully subsonic. The distribution of Pitot pressure, on the cross-sectional plane at a given x , were analyzed and integrated to obtain the axial mass flow rate ('mass flux'), m . In the calculation, the static pressure was assumed to be the same as ambient pressure. In the integration, the 'potential tails' were truncated where the Mach number dropped below 1% of the local centerline Mach number. These considerations have been discussed in the cited references (Refs. 2,3) and are not repeated here.

3. Results

3.1 Jet spreading increase: Schlieren photographs of the flowfield are shown in Fig. 1 for the circular nozzle with and without tabs. The picture at the bottom, for four delta-tabs, illustrates the increase in jet spreading and mixing caused by the tabs. The shock/expansion structures, seen for the no-tab case on the top, are also weakened drastically by the tabs. It should be noted that the flow without the tabs is underexpanded and undergoes a strong self-excitation due to screech. It is expected that such self-excitation cause a higher jet spreading compared to a fully expanded case had there been no screech. The tabs elimi-

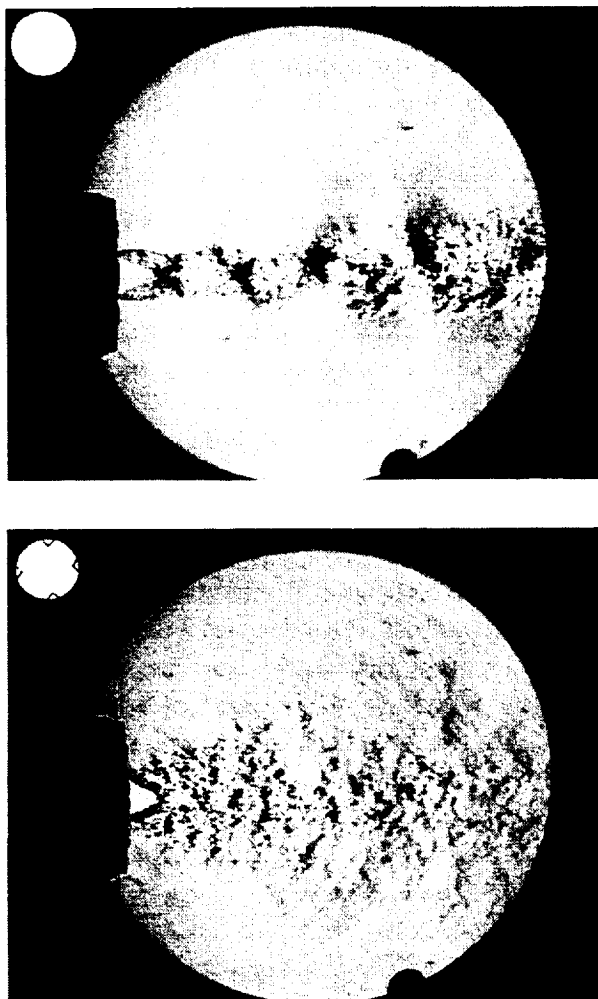


Fig. 1 Schlieren photograph of jet from circular nozzle with and without four delta-tabs; $M_j = 1.63$.

nate screech and yet increase the jet spreading. The tab effect is due primarily to the dynamics of the stream-wise vortex pairs introduced in the flow.²

An assessment of the effect of screech on jet spreading can be made from Fig. 2. Normalized mass flux variation, measured at a fixed downstream location ($x/D_e = 14$), is shown at the bottom of this figure. The experimental data are for the convergent circular nozzle. The measured screech frequency variation is shown on the top. The annotations in the top figure identify screech stages that are well known (e.g., Ref. 5). Here, stages A_1 and A_2 involve axisymmetric, B and D involve flapping, and C involves helical flow oscillations. The mass flux

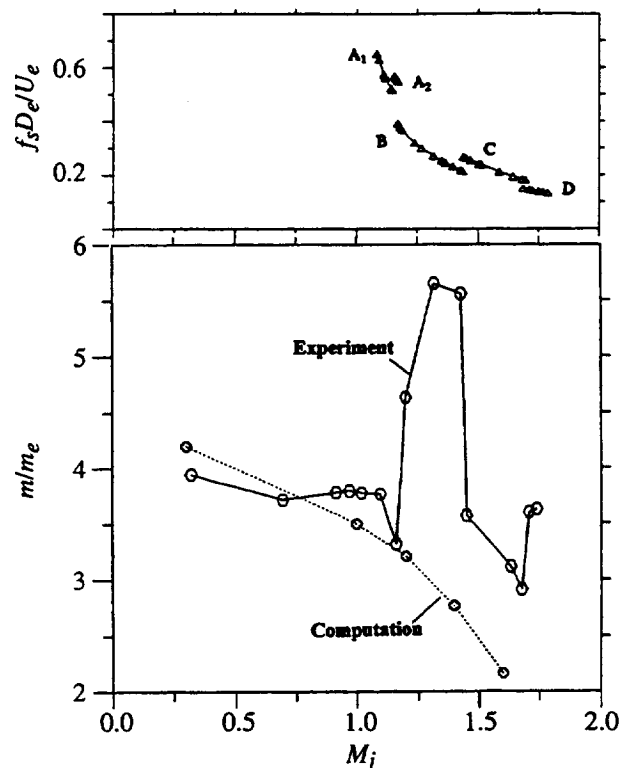


Fig. 2 Normalized mass flux, at $x/D_e = 14$, versus M_j for the circular nozzle, Nondimensional screech frequency is shown on the top.

data can be seen to undergo large variations with M_j , having apparent correlation with the screech stages. The fluxes are highest in the flapping mode B, and are again relatively high in the next flapping mode D. With the onset of the helical mode C, the flux values drop substantially. These results are in agreement with the observations of Glass⁶ and Sherman *et al.*⁷. The drop in the 'impact pressure', at a fixed point on the jet centerline, was observed by them to be the most at pressure ratios that would correspond to the B mode. It should be noted that screech amplitude is known to be sensitive to the nozzle geometry, e.g., the lip thickness.⁸ The amplitude is likely to affect the flux values. Thus, with a different nozzle the fluxes may not be repeatable, however, the trend with varying screech stages may remain the same.

It is reasonable to infer that had there been no screech, the flux values in the supersonic regime would be lower. The steady-state computational results in Fig. 2 provide an idea about the expected trend had there been no screech. The computations were performed by C. J. Steffen and D.R. Reddy; see Steffen *et al.*⁹. Questions remain re-

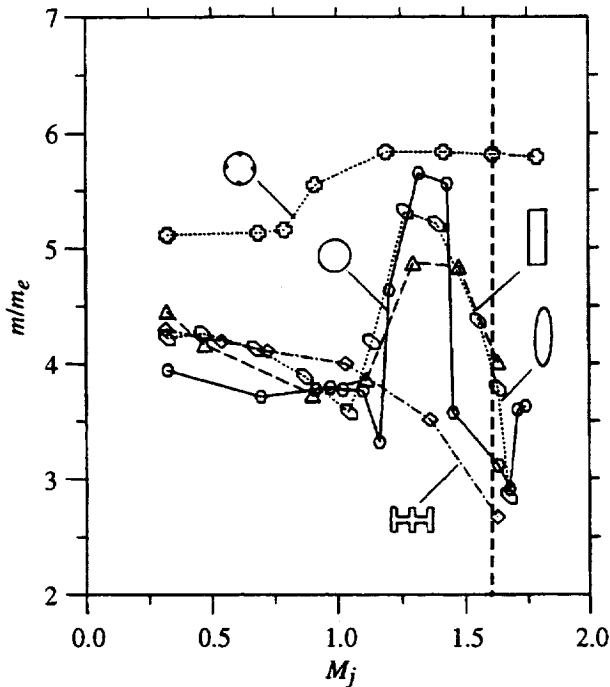


Fig. 3 Normalized mass flux, at $x/D_e = 14$ versus M_j for six nozzle cases.

garding the fidelity of the results; see, also Reddy *et al.*¹⁰. However, it is apparent that screech generally increases jet spreading and the effect is most pronounced in the flapping modes.

Corresponding mass flux data for the three asymmetric nozzles and the tabbed case are compared in Fig. 3. The elliptic and rectangular jets also go through flapping mode screech in the supersonic regime. As a result, variations similar to the circular jet B mode are observed with both nozzles. The complex effect of screech may be appreciated by comparing the flux values at, say, $M_j \approx 1.6$ (marked by the vertical line). First, at this M_j , the fluxes for the elliptic and the rectangular jets are essentially identical but significantly higher than that for the circular jet. A reason for this difference is the difference in the screech modes. Whereas the two asymmetric nozzles involve flapping mode (B), the circular jet involves the helical mode (C), screech. The latter mode, as seen in the previous figure, involves smaller jet spreading. Second, with the lobed nozzle, at the given M_j , the flux value is the lowest among all cases. This result can be attributed to the fact that there is no screech

with the lobed nozzle. Finally, as stated earlier, the tab case is seen to involve the highest spreading in spite of the absence of screech; here a different mechanism is in play, that of the streamwise vortex pairs, causing the increased spreading.

In the low subsonic regime, the fluxes for the asymmetric nozzles are found to be generally higher than that for the circular case. However, these are not significantly higher (no more than 10%). This result contrasts some previous observations,^{11,12} that reported much higher jet spreading with small aspect ratio elliptic nozzles. This led to a further investigation.

An underlying concept with an asymmetric (e.g., lobed) nozzle is to stretch the perimeter of the shear layer so that the interfacial area between the high- and low-speed streams is increased. This is expected to increase mixing. A simple way to stretch the perimeter would be to increase the aspect ratio (AR) of a rectangular nozzle while keeping the area the same. This was done with the orifice cases. An advantage with the orifices, instead of nozzles, was that streamwise vorticity due to upstream secondary flow would be minimal, thus, jet spreading simply due to the shear layer perimeter stretching could be studied.

The mass flux variations obtained with the orifices, at $M_j = 0.95$, are shown in Fig. 4. It can be seen that for AR up to 8:1, the jet spreading has essentially remained the same and is basically indistinguishable from the data obtained with the circular nozzle. Only when AR is increased to 16, does an increase in the jet spreading finally occur. As expected, the effect becomes clearly pronounced with even larger AR (32:1). These results suggest that the effect of shear layer perimeter stretching must be insignificant for small aspect ratio asymmetric nozzles.

What then caused the large entrainment in the low aspect ratio elliptic jets reported in the literature (e.g., Refs. 11,12)? A difference in the initial condition, i.e., initial boundary layer state, is thought to be a likely reason for this difference. At $M_j \geq 0.3$ with the present jets, the initial boundary layer was 'nominally laminar' and the fluctuation intensity was high with a broadband spectrum. At low Mach and Reynolds numbers in the jets of Ho & Gutmark¹¹ and Hussain & Husain¹², the initial boundary layer was laminar and the turbulence was low. One may conjecture that the latter jets are susceptible to small amplitude background disturbances. It is as though these jets are prone to

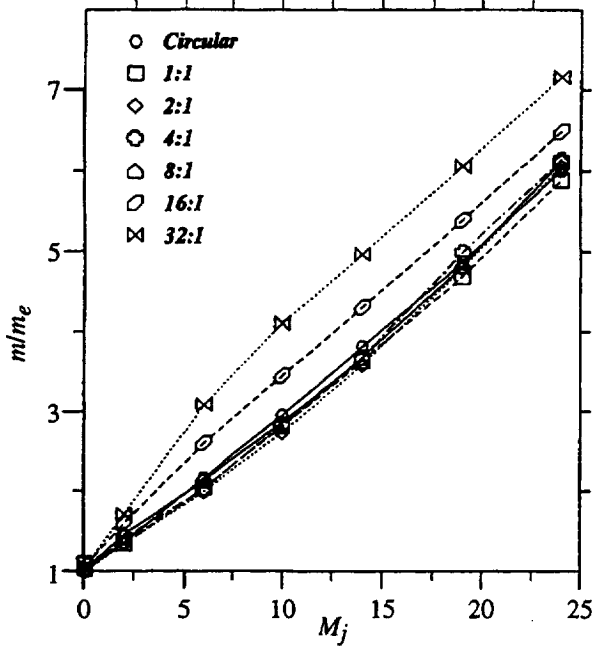


Fig. 4 For $M_j = 0.95$, streamwise variation of normalized mass flux for the rectangular orifice cases; 'circular' represents circular nozzle data.

'self excitation', and there can be an organized roll up of the azimuthal vorticity similar to what happens with an artificially excited jet. This would lead to a higher spreading and entrainment through the self-induction and dynamics of the asymmetric vortex rings, (see, e.g., Refs. 11-13). This initial condition effect was vividly illustrated by the data of Hussain & Husain.¹² When they tripped the boundary layer of their elliptic nozzle the spreading was significantly less (their figure 32). Therefore, a relatively 'unclean' initial condition with the present jets, practically inevitable at higher jet Mach numbers, is thought to be responsible for the lesser jet spreading. It should be emphasized that the latter initial condition would be expected in most 'industrial-type' applications. Therefore, simply small-aspect-ratio rectangular or elliptic nozzles may not be efficient flow mixers in those situations.

Another factor that might make a difference in jet spreading with asymmetric nozzles is streamwise vorticity distribution at the nozzle exit. Any nozzle contracting from one cross-sectional shape to another would be characterized by such vortices due to upstream secondary flow. The strength and sense of rotation of the vor-

tices would depend on the detailed geometry of the nozzle. The initial streamwise vorticity distribution can impact the jet evolution significantly. As stated earlier, the large spreading increase observed with the tabs is due to the dynamics of the streamwise vortex pairs. Streamwise vorticity generation by the tabs and the subsequent dynamics of the vortex pairs have been adequately discussed earlier (see, Refs. 2, 14-16) and these are not repeated here. The spreading increase vis-à-vis the thrust penalty caused by the tabs is addressed next.

3.2 Flow blockage and thrust loss due to the tabs: Thrust data for several tab cases have been presented in Ref. 2. The data for four delta-tabs with the circular nozzle are further examined here. Thrust was measured by a 'load-cell' with the plenum chamber mounted on linear bearings. Simultaneously, the mass flow rate was also measured by an orifice-meter installed on the air supply line.

The ideal mass flow rate for the nozzle, m_{ideal} $= \rho_e A_e U_e$, was calculated from conditions at the nozzle exit assuming a uniform velocity profile and zero boundary layer thickness. The subscript 'e' denotes conditions at the exit that were calculated from the plenum-chamber-to-ambient pressure ratio. Comparison with the measured mass flow rate, m_{meas} , provided the actual flow blockage (blockage $= (m_{ideal} - m_{meas})/m_{ideal}$). For the purposes of analyzing the tab cases, an equivalent exit area, $A_{eq} = m_{meas} / \rho_e U_e$, was calculated from the measured mass flow rate. (Note that the equivalent diameter, D_e , was based on the exit cross-sectional area, A_e , of the nozzle. The diameter, D_{eq} , used in table 1 is based on A_{eq} .) The area A_{eq} (or A_e for the no-tab cases) was then used to calculate an ideal thrust, F_{ideal} , via the equation,

$$F_{ideal} = A_{eq} \rho_e U_e^2 + (p_e - p_a) A_{eq}, \quad (1)$$

For the given p_0 , p_a and A_{eq} , the maximum available thrust F_{max} , was calculated via the equation,¹⁷

$$F_{max} = p_0 A_{eq} \left[\frac{2}{\gamma - 1} \left(\frac{2}{\gamma + 1} \right)^{\frac{\gamma + 1}{\gamma - 1}} \left(1 - \left(\frac{p_a}{p_0} \right)^{\frac{\gamma - 1}{\gamma}} \right) \right]^{1/2} \quad (2)$$

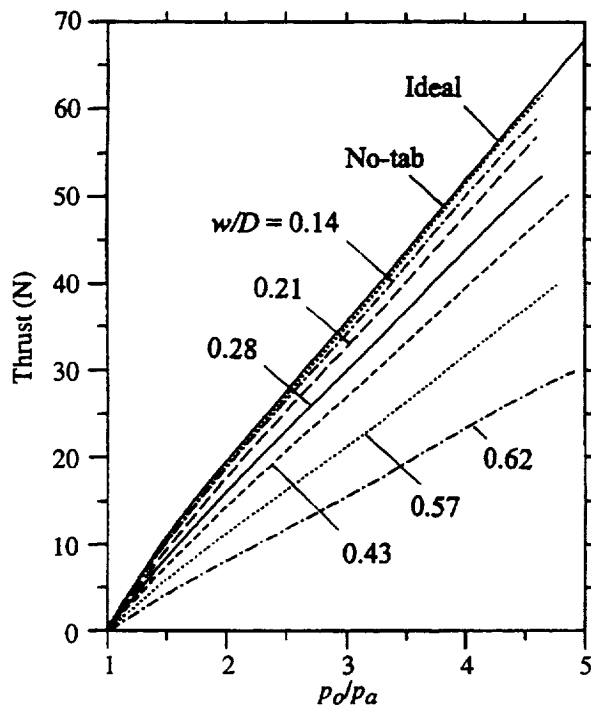


Fig. 5 Thrust versus pressure ratio for the convergent circular nozzle with and without 4 delta-tabs, for varying tab size w/D_e (table 1).

The thrust coefficients C_f and C_{f0} were then calculated as,

$$C_f = F_{meas}/F_{ideal}, \text{ and, } C_{f0} = F_{meas}/F_{max}.$$

Note that F_{ideal} is the thrust for the given pressures for a given nozzle geometry assuming ideal flow. On the other hand, F_{max} is the maximum available thrust that would be obtained by fully expanding the flow with a C-D nozzle of same throat area, $A_t (=A_{eq})$, but an appropriately larger exit area, A_e .

The measurements were performed for a given tab configuration followed by normalized mass flux measurement at $x/D_{eq} = 14$ (data as in Fig. 3). The sequence of measurement was repeated with the four equally spaced delta-tabs, the tab size having been varied. The base width of the tab (w/D_e) was varied as, 0.14, 0.21, 0.28, 0.43, 0.57 and 0.62. These are listed as cases 2 through 7 in table 1, case #1 being without tabs.

The measured thrust for cases 1-7 is shown in Fig. 5 as a function of the nozzle pressure ratio (p_0/p_a).

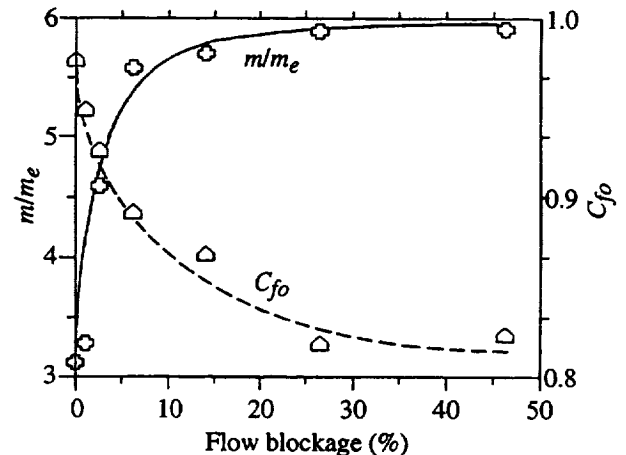









Fig. 6 Effect of four delta tabs of varying size on the mass flux (at $x/D_{eq} = 14$) and the thrust coefficient of the circular jet. Abscissa is measured flow blockage for the seven cases of table 1.

The curve marked 'ideal' represents ideal thrust for the no-tab case assuming zero boundary layer thickness. The slightly lower thrust measured for this case should be due to the boundary layer effect. (Note that the flow in the supersonic regime is underexpanded and thus, $F_{ideal} < F_{max}$; see further discussion later.) It is evident that with increasing size of the tabs there is increasing thrust loss. The measured loss relative to the ideal value in percent is listed in column 5 of table 1.

With increasing tab size, the flow rate also decreases for a given pressure ratio. The measured flow blockage is listed in column 4 of table 1. The flow blockage and thrust loss, calculated for $p_0/p_a = 4.47$ ($M_j = 1.63$), are representative of corresponding values at other pressure ratios. Since the thrust loss is accompanied by a decrease in mass flow rate, an evaluation of the performance is appropriate only when the thrust coefficient is compared. The coefficient, C_{f0} , is listed in column 6 of table 1. Note that in Ref. 2, corresponding values of C_f were reported. In the underexpanded supersonic regime $C_f > C_{f0}$, since $F_{ideal} < F_{max}$; (for example, at $M_j = 1.63$ for the convergent nozzle, $F_{ideal}/F_{max} = 0.977$). The variation of C_{f0} for cases 1-7 is shown in figure 6. The flow blockage, representing the size of the tabs, is arbitrarily chosen as the abscissa. A steep initial decrease in C_{f0} with increasing tab size is apparent. But with further increase in the size the curve levels off.

Table 1 Flow blockage, jet spreading and thrust loss for four delta-tabs with the circular nozzle, at $M_j = 1.63$.

Case	Tab configuration	Tab base width, w/D_e	Flow blockage (%)	Thrust loss (%)	Thrust co-efficient, $C_f \eta$	Mass flux m/m_e at $x/D_{eq} = 14$	Peak Mach number at $x/D_{eq} = 14$	Performance factor
1	No tab 	0	0	0	0.977	3.12	0.86	--
2	4 delta 	0.14	1.1	4.0	0.949	3.28	0.79	1.0
3		0.21	2.6	7.6	0.926	4.59	0.58	6.4
4		0.28	6.2	15.6	0.892	5.58	0.50	7.3
5		0.43	14.1	23.7	0.869	5.70	0.47	6.3
6		0.57	26.5	38.4	0.819	5.89	0.42	4.9
7		0.62	46.3	54.7	0.824	5.91	0.37	5.1

As discussed earlier,^{14,15} each tab produces a pair of streamwise vortices. The generation of streamwise vorticity represents diversion of some of the axial momentum into circulation on the cross-stream plane. Hence, there is an accompanying drop in the thrust coefficient. With increasing size of the delta-tab the magnitude of the circulation, for each 'leg' of the vortex pair, is expected to increase. This expectation is based on experimental evidence that the nondimensional circulation is a constant. The circulation, nondimensionalized by the approach velocity and the base width of the delta-tab, was measured to be about 0.1 by Foss & Zaman.¹⁶ Corresponding values estimated from streamwise vorticity distribution, for an order of magnitude larger tab by Bohl and Foss,¹⁵ and for an order of magnitude smaller tab by Zaman *et al.*,¹⁴ were about the same. Thus, with increasing tab size the circulation is expected to increase for a given jet velocity. This would be accompanied by a decrease in $C_f \eta$. This qualitatively explains the observed decrease in the thrust coefficient.

The normalized mass flux data, for $x/D_{eq} = 14$, are also shown in Fig. 6. These data exhibit a trend that is the reverse of what occurs with $C_f \eta$. There is a sharp increase in m initially but the rate of increase falls off with further increase in the tab size. The curve levels off

for tab base width (w/D_e) larger than about 0.28 (blockage of about 6%).

Thus, with increasing tab size, the streamwise vortices and the associated circulation on the cross-stream plane become stronger. Stronger cross-stream circulation yield increased jet spreading. But this is achieved at the expense of thrust loss. Furthermore, for a given nozzle, the tab size (w/D_e) can be increased only up to a limit. Beyond that, there is flow interference from adjacent tabs causing a decrease in the strength of the circulation. (Such an effect on circulation due to interference from tabs placed too close to each other was reported in ref. 16). Thus, both the rate of increase in jet spreading and the rate of decrease in $C_f \eta$ decrease as the tab size becomes large.

The increase in spreading versus the loss in thrust is described by a 'performance factor' listed in the last column of table 1. This quantity, defined as,

$$p.f. = \left(\frac{m_{tab} - m_{no-tab}}{m_{no-tab}} \right) / (1 - C_{f0}), \quad (3)$$

represents the percent increase in the mass flux at $x/D_{eq} = 14$ per percent decrease in the thrust co-efficient. It is used to summarize the overall effect but the reader is cautioned not

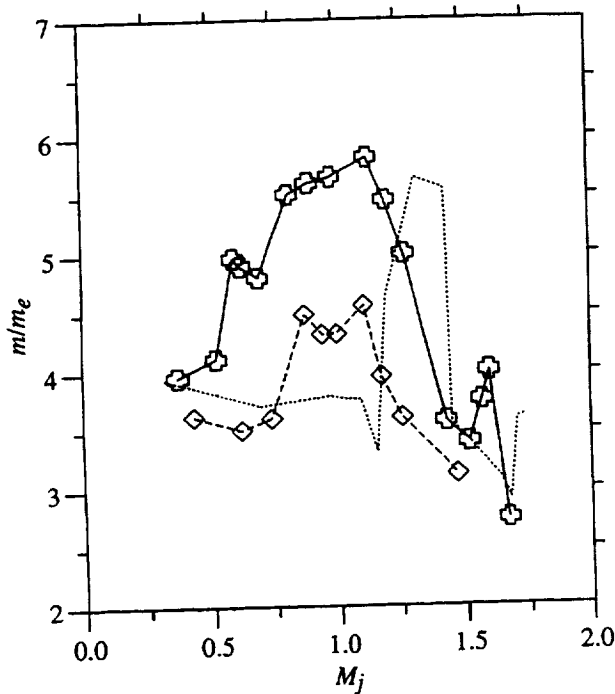


Fig. 7 Normalized mass flux, at $x/D_e = 14$, versus M_j for circular C-D nozzle; \circ , $M_D = 1.8$ nozzle; \diamond , $M_D = 1.4$ nozzle; dotted line, convergent nozzle (Figs. 2 and 3).

to put too much emphasis on it, since with the tab size approaching zero it becomes indeterminate. Note, again, that the performance factor was calculated based on C_f instead of C_{f0} in Ref. 2; as a result the reported values were larger, however, the trend was the same. Based on this factor it is apparent that the optimum size, for the four delta-tabs with the circular nozzle, is in the range $0.21 < w/D_e < 0.28$.

3.3 Spreading increase and thrust loss due to overexpansion: Let us now examine the effect of overexpansion on jet spreading with the convergent-divergent nozzles. Mass flux data, at $x/D_e = 14$, for the two C-D nozzles are compared to the data for the convergent nozzle in Fig. 7. With both C-D nozzles, an increase in the normalized flux occurs over a large range around $M_j = 1$. As further elaborated in the following, the flow in most of this range for either nozzle is in a state of overexpansion. The increase with the $M_D = 1.8$ nozzle is quite large, larger than that achieved by the B-mode screech with the convergent nozzle. The effect observed with the C-D nozzles is further explored.

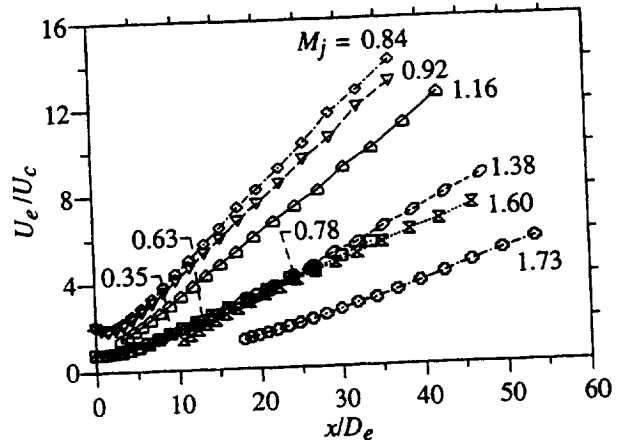


Fig. 8 Streamwise variations of centerline mean velocity (U_c , shown as U_e/U_c) for different M_j ; $M_D = 1.8$ C-D nozzle.

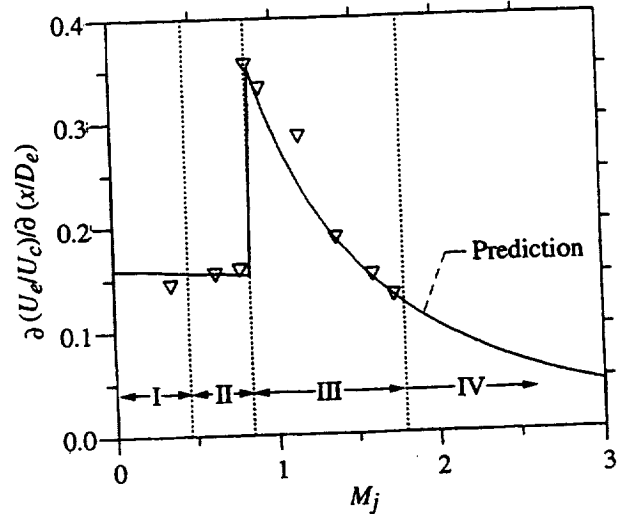


Fig. 9 Asymptotic slopes of U_e/U_c vs. x/D_e as a function of M_j ; C-D nozzle with $M_D = 1.8$.

First, overall characteristics of the jets from the $M_D = 1.8$ nozzle are examined. The variations of the centerline velocity (U_c) are shown in Fig. 8 for several M_j . Inverse of U_c normalized by the velocity at the exit (U_e) is plotted as a function of x/D_e . Here, U_e is calculated from the pressure ratio and the throat-to-exit area ratio and based on one-dimensional nozzle flow analysis. It can be seen that the slopes of these curves are large around $M_j = 1$ indicating a faster jet spreading.

The asymptotic slopes of the U_e/U_c curves in Fig. 8 are plotted in Fig. 9, as a function of M_j . In this figure, the

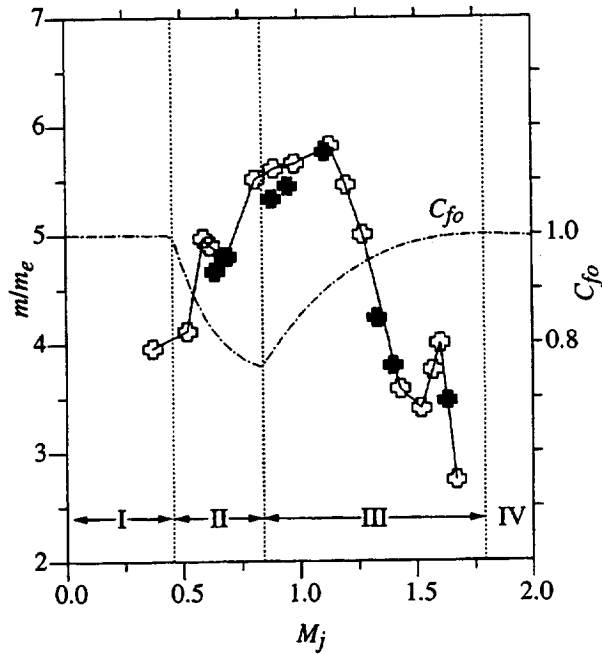


Fig. 10 Normalized mass flux, at $x/D_e = 14$, versus M_j for $M_D = 1.8$ C-D nozzle. Solid symbol: for boundary layer trip near throat. Chain-dashed line: ideal thrust coefficient.

vertical lines demarcate flow regimes I-IV based on one-dimensional flow analysis. Regime 'I' denotes the range where the flow is subsonic throughout; 'II', when a normal shock is expected within the diverging section of the nozzle; 'III', when the flow is overexpanded; and 'IV', when the flow is underexpanded. The asymptotic slopes can be predicted based on conservation of momentum and dimensional reasonings as,

$$U_e/U_c = C_2 \xi^{-1/2} (\rho_a/\rho_e)^{1/2} (x/D_e), \quad (4)$$

where, $\xi = 1 + (p_e - p_a)/\rho_e U_e^2$, and C_2 is a constant. For incompressible flow, the coefficient on the right of Eq. (4), ($C = C_2 \xi^{-1/2} (\rho_a/\rho_e)^{1/2}$), is approximately 0.16. The curve marked prediction in Fig. 9 represents Eq. (4) with the value matched to 0.16 at $M_j = 0$. At higher M_j , ξ and ρ_e are calculated to obtain the rest of the curve. Details of this analysis can be found in Ref. 3.

It is clear from Fig. 9 that the asymptotic slopes agree quite well with the prediction. The prediction hinges on the correct calculation of the exit parameters (U_e , p_e , ρ_e , etc.), and these are obtained by assuming idealized one-dimensional flow. The agreement of the data with the prediction provides the confidence that the flow through the nozzle is 'well behaved', and that there may not be any peculiarities, e.g., significant boundary layer separation within the nozzle. The calculated exit parameters provide the initial mass flux and jet thrust that are pertinent in the following discussion.

The flux data for the $M_D = 1.8$ nozzle are now further examined in Fig. 10. Flow regimes I-IV are shown in this figure. The open data points are reproduced from Fig. 7. The solid data points are obtained with the boundary layer tripped near the throat of the nozzle. The significance of the tripped case is as follows.

With a smooth interior, C-D nozzles often undergo a flow resonance with accompanying tone(s) in the overexpanded regime. This phenomenon, easily confused with screech tones, is indeed quite different in origin. It has been traced and linked to unsteady boundary layer separation near the throat of the nozzle,¹⁸ and suitable boundary layer tripping would eliminate the tone completely. Both C-D nozzles employed in the present study involve such tones in the range of M_j where the enhanced spreading is observed. The solid symbols in Fig. 10 represent the condition where the tone is eliminated by boundary layer tripping. It should be clear that the observed increase in the flux is not due to the flow resonance and accompanying self-excitation. (Only the slightly larger values with the open symbols are apparently due to the additional effect of the self-excitation.) Thus, the spreading increase seen in the overexpanded regime must be due to other factors which, unfortunately, remain unclear at this time.

The thrust loss in the overexpanded regime, accompanying the increased spreading, is considered now. Unlike with the tabs, thrust could not be measured for these C-D nozzles due to facility limitations. Thrust was calculated with the assumption of idealized nozzle flow. The ideal and maximum thrusts (F_{ideal} and F_{max}), for a given p_0 and p_a were calculated via Eqs. (1) and (2); the throat area of the nozzle, A_t , replaced A_{eq} . Assuming actual thrust to be F_{ideal} , C_{fo} ($=F_{ideal}/F_{max}$) was then calculated for different pressure ratio (M_j). This is plotted in Fig. 10.

With increasing M_j the thrust coefficient is found to decrease in regime II where a normal shock is expected in the diverging section. It reaches the minimum at the onset of the overexpanded regime. With further increase in pressure ratio, $C_f\eta$ increases and reaches a value of unity at the design condition ($M_j = 1.8$). Then as the flow becomes underexpanded (Regime IV), a gradual decrease in the value of $C_f\eta$ commences. The results in Fig. 10 show that whereas the minimum value of $C_f\eta$ is expected at the beginning of the overexpanded regime the maximum increase in the spreading takes place at a higher M_j , well into the overexpanded regime. A similar observation can be made with the other ($M_D = 1.4$) nozzle for which the corresponding data are shown in figure 11. With the latter nozzle, both the increase in the mass flux and the decrease in $C_f\eta$ are smaller compared to the corresponding values with the $M_D = 1.8$ nozzle.

The 'performance factor' (Eq. 3) is evaluated for the effect of overexpansion with the $M_D = 1.8$ nozzle. (For the other C-D nozzle, as discussed in the previous subsection, the performance factor tends to be indeterminate and is ignored.) Note that the maximum spreading occurs around $M_j = 1.1$, whereas the values shown in table 1 for the tab cases pertain to $M_j = 1.63$. At $M_j = 1.1$, the performance factor for the optimum tab case ($w/D_e = 0.28$) can be estimated to be 4.9 (the flux values are obtained from Fig. 3 and $C_f\eta$ is assumed to be the same as in table 1, 0.892). Corresponding performance factor for the $M_D = 1.8$ nozzle, at $M_j = 1.1$, turns out to be 5.3. Thus, the optimum 'performance' with the overexpansion is comparable or slightly better than that with the four delta-tabs. Note, however, that thrust is calculated for the overexpansion case assuming idealized flow. Actual thrust and $C_f\eta$ are likely to be somewhat lower. Finally, it should be emphasized that only limited exploration has been done with the C-D nozzles and it is possible that other design conditions exist that may perform better. On the other hand, it is also possible that other configurations of vortex generators and tabs exist that may have better performance.

4. Concluding Remarks:

Several 'passive control' techniques have been studied for comparative effectiveness in terms of mixing

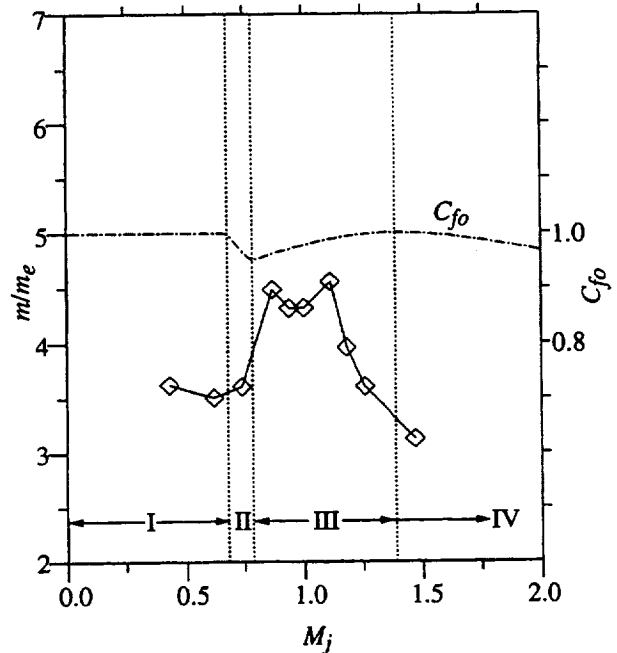


Fig. 11 Normalized mass flux, at $x/D_e = 14$, versus M_j for $M_D = 1.4$ C-D nozzle. Chain-dashed line: ideal thrust coefficient.

and spreading enhancement in free jets. Screech tones increase jet spreading. The increase depends on the characteristic mode of the screech. Compared to axisymmetric or helical modes, flapping mode screech leads to a larger jet spreading.

For asymmetric nozzles, it is demonstrated that the increase in jet spreading due to 'shear layer perimeter stretching' is negligible. The results suggest that small-aspect-ratio rectangular or elliptic nozzles, by themselves, may not be efficient flow mixers. However, introduction of streamwise vortices or some form of unsteady excitation with these nozzles can lead to efficient mixing and large spreading.

The state of overexpansion with convergent-divergent nozzles also leads to an increased jet spreading. It is shown that this effect is not due to a self-excitation caused by flow resonance that is some times encountered in the overexpanded regime. The actual mechanism remains unclear. One may speculate that the observed increase in spreading occurs due to prevalent pressure gradients. The pressure at the nozzle exit is lower than the ambient and depends on the state of overexpansion. Thus, the initial

region of the jet is subjected to pressure gradients in the streamwise as well as lateral directions. This may not only affect momentum transfer in the lateral direction but also the stability characteristics of the shear layers.

Consistently large jet spreading is achieved with the tabs, in subsonic as well as supersonic regimes. However, the tabs involve thrust penalty. Measured thrust coefficients are evaluated in comparison to the increase in the jet spreading. For four equally spaced delta-tabs with the circular nozzle, optimum performance is achieved when the tab size is such that the base width, w/D_e , is in the range 0.21 - 0.28. For this size, the 'performance factor', defined as the ratio of increase in the mass flux at a given downstream location to decrease in the thrust coefficient, attains the maximum value. Comparable spreading increase and performance are also achieved with overexpanded flow for the $M_D = 1.8$ C-D nozzle.

Finally, it should be noted that the spreading increase achieved by screech, even though not as large as that achieved by the tabs or overexpansion, is still quite significant in the B-mode. The corresponding thrust data indicate that the associated loss may be negligible and, in fact, indistinguishable from the loss due to boundary layer skin friction (compare the data for the no-tab case with the ideal case in Fig. 5). This suggests that, in terms of 'active control', unsteady flapping mode excitation may be attractive for further exploration.

References:

1. Gutmark, E.J., Schadow, K.C. & Yu, K.H., 1995, "Mixing enhancement in supersonic free shear flows", *Annual Review Fluid Mech.*, 27, pp. 375-417.
2. Zaman K.B.M.Q., 1999, "Spreading characteristics of compressible jets from nozzles of various geometries", *J. Fluid Mech.*, 383, pp. 197-228.
3. Zaman K.B.M.Q., 1998, "Asymptotic spreading rate of initially compressible jets - experiment and analysis", *Physics of Fluids*, 10, pp. 2652-2660.
4. Panda, J., 1995, "Measurement of shock oscillation in underexpanded supersonic jets", *AIAA Paper* 95-2145.
5. Powell, A., Umeda, Y. & Ishii, R., 1990, "The screech of round choked jets, revisited", *AIAA Paper* 90-3980.
6. Glass, D.R. , 1968, "Effects of acoustic feedback on the spread and decay of supersonic jets", *AIAA J.*, 6(10), pp. 1890-1897.
7. Sherman, P.M., Glass, D.R. & Duleep, K.G., 1976, "Jet flow field during screech", *Applied Sci. Res.*, 32(3), pp. 283-303.
8. Raman, G. 1997, "Cessation of screech in underexpanded jets", *J. Fluid Mech.* 336, pp. 69-90.
9. Steffen, C.J., Reddy, D.R. & Zaman, K.B.M.Q., 1997, "Numerical modeling of jet entrainment for nozzles fitted with delta tabs", *AIAA Paper* 97-0709, 35th Aerospace Sciences Meeting, Reno, NV.
10. Reddy, D.R., Steffen, C.J. & Zaman, K.B.M.Q., 1997, "Computation of 3-D compressible flow from a rectangular nozzle with delta tabs", *Paper* 97-GT-257, *ASME Gas Turbine Conf.*, Orlando.
11. Ho C.-M. & Gutmark E. , 1987, "Vortex induction and mass entrainment in a small-aspect-ratio elliptic jet", *J. Fluid Mech.*, vol. 179, pp. 383-405.
12. Hussain F. & Husain H.S., 1989, "Elliptic jets. Part 1. Characteristics of unexcited and excited jets", *J. Fluid Mech.*, vol. 208, pp. 257-320.
13. Grinstein, F., 1995, "Self-induced vortex ring dynamics in subsonic rectangular jets", *Physics of Fluids*, 7 (10), pp. 2519-2521.
14. Zaman K.B.M.Q., Reeder M.F., & Samimy M., 1994, "Control of an axisymmetric jet using vortex generators", *Physics of Fluids A*, 6 (2), pp. 778-793.
15. Bohl, D. & Foss, J., 1999, "Near exit plane effects caused by primary and primary-plus-secondary tabs", *AIAA J.*, 37 (2), pp. 192-201.
16. Foss, J.K. & Zaman, K.B.M.Q., 1999, "Large and small scale vortical motions in a shear layer perturbed by tabs", *J. Fluid Mech.*, (to appear).
17. Shapiro, A.H., "The dynamics and thermodynamics of compressible fluid flow", *The Ronald Press Co.*, New York, 1953.
18. Zaman, K.B.M.Q. and Dahl, M. D., 1999, "Aeroacoustic resonance with convergent-divergent nozzles", *AIAA paper* 99-0164, 37th Aerospace sciences Meeting, Reno, NV.

